BJP British Journal of Pharmacology

DOI:10.1111/bph.12117
www.brjpharmacol.org

Themed Issue: Histamine Pharmacology Update

RESEARCH PAPER

Detailed analysis of biased histamine H_4 receptor signalling by JNJ 7777120 analogues

S Nijmeijer[1], H F Vischer[1], F Sirci[2], S Schultes[1], H Engelhardt[1], C de Graaf[1], E M Rosethorne[3], S J Charlton[3] and R Leurs[1]

[1]*Division of Medicinal Chemistry, Faculty of Sciences, Amsterdam Institute for Molecules, Medicines and Systems (AIMMS), VU University Amsterdam, Amsterdam, The Netherlands,* [2]*Laboratory for Chemometrics and Chemoinformatics, Chemistry Department, University of Perugia, Perugia, Italy, and* [3]*Novartis Institutes for Biomedical Research, Horsham, UK*

Correspondence
Rob Leurs, Division of Medicinal Chemistry, Faculty of Sciences, Amsterdam Institute for Molecules, Medicines and Systems (AIMMS), VU University Amsterdam, De Boelelaan 1083, 1081 HV Amsterdam, The Netherlands. E-mail: r.leurs@vu.nl

Keywords
biased ligands; histamine H_4 receptor; β-arrestin; indolecarboxamides; FLAP 3D-QSAR; efficacy; intrinsic activity; efficacy hotspots

Received
27 November 2012
Revised
26 December 2012
Accepted
2 January 2013

BACKGROUND AND PURPOSE

The histamine H_4 receptor, originally thought to signal merely through $G\alpha_i$ proteins, has recently been shown to also recruit and signal via β-arrestin2. Following the discovery that the reference antagonist indolecarboxamide JNJ 7777120 appears to be a partial agonist in β-arrestin2 recruitment, we have identified additional biased hH_4R ligands that preferentially couple to $G\alpha_i$ or β-arrestin2 proteins. In this study, we explored ligand and receptor regions that are important for biased hH_4R signalling.

EXPERIMENTAL APPROACH

We evaluated a series of 48 indolecarboxamides with subtle structural differences for their ability to induce hH_4R-mediated $G\alpha_i$ protein signalling or β-arrestin2 recruitment. Subsequently, a Fingerprints for Ligands and Proteins three-dimensional quantitative structure–activity relationship analysis correlated intrinsic activity values with structural ligand requirements. Moreover, a hH_4R homology model was used to identify receptor regions important for biased hH_4R signalling.

KEY RESULTS

One indolecarboxamide (**75**) with a nitro substituent on position R7 of the aromatic ring displayed an equal preference for the $G\alpha_i$ and β-arrestin2 pathway and was classified as unbiased hH_4R ligand. The other 47 indolecarboxamides were β-arrestin2-biased agonists. Intrinsic activities of the unbiased as well as β-arrestin2-biased indolecarboxamides to induce β-arrestin2 recruitment could be correlated with different ligand features and hH_4R regions.

CONCLUSION AND IMPLICATIONS

Small structural modifications resulted in diverse intrinsic activities for unbiased (**75**) and β-arrestin2-biased indolecarboxamides. Analysis of ligand and receptor features revealed efficacy hotspots responsible for biased-β-arrestin2 recruitment. This knowledge is useful for the design of hH_4R ligands with biased intrinsic activities and aids our understanding of the mechanism of H_4R activation.

LINKED ARTICLES

This article is part of a themed issue on Histamine Pharmacology Update. To view the other articles in this issue visit http://dx.doi.org/10.1111/bph.2013.170.issue-1

Abbreviations

CRE, cyclic AMP response element; FLAP, Fingerprints for Ligands and Proteins; hH_4R, human histamine H_4 receptor; MIF, molecular interaction fields; TM, transmembrane

Introduction

GPCRs are attractive therapeutic targets. Their presence on the cell surface allows extracellular molecules to bind and stabilize active GPCR conformations that can subsequently provoke intracellular responses. Although the overall folding of GPCRs has been known for quite a while, three-dimensional (3D) structures of several family members have

only recently been elucidated (Palczewski *et al.*, 2000; Jaakola *et al.*, 2008; Warne *et al.*, 2008; Wu *et al.*, 2010; Rasmussen *et al.*, 2011b; Shimamura *et al.*, 2011; Granier *et al.*, 2012; Haga *et al.*, 2012; Manglik *et al.*, 2012). This breakthrough was one of the main reasons why the Nobel Prize 2012 for chemistry has been awarded to Drs Robert Lefkowitz and Brian Kobilka for their pioneering work on GPCRs. Knowledge on ligand–receptor interactions and their downstream effects is important to design specific compounds with less side effects (Galandrin *et al.*, 2007). Both inactive and active GPCR structures are currently available but we are not yet able to predict ligand efficacy on the design table. This prediction is further complicated by the realization that multiple active receptor conformations exist, which couple to multiple downstream effector proteins and pathways with distinct propensities (Kenakin, 2003; Bohn and McDonald, 2010; Reiter *et al.*, 2012). The idea that some ligands may preferentially stabilize different conformation led to the identification of biased ligands, in which an agonist in pathway A can be an antagonist in pathway B (Violin *et al.*, 2010). Biased GPCR signalling clearly further complicates drug discovery efforts, but also holds the promise to design specific biased ligands that antagonize adverse signalling routes while stimulating beneficial responses (Rajagopal *et al.*, 2010; DeWire and Violin, 2011; Kenakin, 2011; Reiter *et al.*, 2012).

The human histamine H_4 receptor (hH_4R) belongs to the class A GPCR family and is considered an important receptor in immune and inflammatory processes (Leurs *et al.*, 2009; Zampeli and Tiligada, 2009). Since its discovery in 2000, the hH_4R has been shown to signal via heterotrimeric $G\alpha_i$ proteins (Nakamura *et al.*, 2000; Oda *et al.*, 2000; Coge *et al.*, 2001; Liu *et al.*, 2001; Morse *et al.*, 2001; Zhu *et al.*, 2001). However, the reference antagonist JNJ 7777120 (Thurmond *et al.*, 2004) was recently identified as partial agonist in a β-arrestin2 recruitment assay (Rosethorne and Charlton, 2011). Subsequent analysis of 31 known H_4R ligands revealed both $G\alpha_i$ protein and β-arrestin2-biased ligands that covered different chemical classes (Nijmeijer *et al.*, 2012). Interestingly, all five tested indolecarboxamides (JNJ 7777120 analogues) in that study were fully biased towards the β-arrestin2 pathway and exhibited partial agonistic activity.

Recently, we developed a series of JNJ 7777120 analogues with subtle chemical switches to optimize their affinity for the hH_4R (Engelhardt *et al.*, 2012). This set of compounds is extremely useful to systematically investigate molecular features responsible for biased hH_4R signalling. In this study, we therefore determined the intrinsic activity of 48 indolecarboxamides in β-arrestin2 recruitment and $G\alpha_i$ signalling, followed by a detailed structure–activity analysis. We were able to identify molecular features that are positively or negatively correlated with the ability of ligands to induce biased hH_4R signalling. The current study is one of the first to use computational analysis (Sirci *et al.*, 2012; Wijtmans *et al.*, 2012) to correlate ligand structures with intrinsic activities. Moreover, with a hH_4R homology model, we could identify receptor regions important for biased hH_4R signalling. This is a promising first step towards the identification of ligand efficacy hotspots that may allow the rational design of ligands with specific GPCR (biased) activity and that will aid the understanding of GPCR activation.

Methods

Materials

Cell culture media used for the HEK293T and U2OS-H4R cells were purchased from PAA (Pasching, Austria) and Invitrogen (Carlsbad, CA, USA) respectively. Forskolin and histamine were bought from Sigma-Aldrich (St. Louis, MO, USA). Synthesis of the indolecarboxamide analogues was previously described (Engelhardt *et al.*, 2012).

Cell culture and transfection

HEK293T cells were cultured in DMEM supplemented with 10% FBS, 50 IU·mL^{-1} penicillin and 50 µg·mL^{-1} streptomycin at 37°C and 5% CO_2. Two million cells were seeded per 10 cm dish 1 day prior to transfection. Approximately four million cells were transfected with 5 µg of cDNA using the polyethyleneimine (PEI) method. Briefly, 2.5 µg hH_4R cDNA was supplemented with 2.5 µg CRE-luc plasmid to a total of 5 µg cDNA and mixed with 20 µg of 25 kDa linear PEI in 500 µL of 150 mM NaCl. This transfection mix was incubated at 22°C for 10–30 min and subsequently added drop-wise to a 10 cm dish containing 6 mL of fresh culture medium. PathHunter™ U2OS β-arrestin2 : EA cells stably expressing the human histamine H_4 receptor (U2OS-H_4R) (Rosethorne and Charlton, 2011) were cultured in minimum essential media (MEM) containing L-glutamine supplemented with FBS (10% v/v), penicillin (100 IU·mL^{-1}), streptomycin (100 µg·mL^{-1}) G418 Geneticin (500 µg·mL^{-1}) and hygromycin (250 µg·mL^{-1}) at 37°C, 5% CO_2. On the day prior to the β-arrestin2 recruitment assay, 10 000 cells per well were seeded in a white, clear bottomed 384 well ViewPlate (Perkin Elmer Life and Analytical Sciences, See Green, Buckinghamshire, UK) in 20 µL MEM supplemented as described previously and incubated at 37°C, 5% CO_2.

CRE (cyclic AMP response element) luciferase reporter gene assay

Transiently transfected HEK293T cells were stimulated for 6 h with indicated indolecarboxamides or DMSO (1%) in serum-free DMEM containing 1 µM forskolin at 37°C, 5% CO_2. Subsequently, the medium was aspirated and 25 µL of luciferase assay reagent [LAR, 0.83 mM ATP, 0.83 mM d-luciferine, 18.7 mM MgCl2, 0.78 µM Na_2HPO_4, 38.9 mM Tris–HCl (pH 7.8), 0.39% glycerol, 0.03% Triton X-100 and 2.6 µM DTT] was added to each well.

Luminescence (1 s per well) was measured in a Victor^3 1420 multi-label reader (Perkin Elmer Life and Analytical Sciences) after 30 min of incubation at 37°C, 5% CO_2.

β-Arrestin2 recruitment assay

U2OS-H_4R cells were stimulated with increasing amounts of indolecarboxamides or DMSO (1%) for 2 h at 37°C, 5% CO_2 in assay buffer (HBSS supplemented with 20 mM HEPES and 0.1% BSA). Directly after stimulation, 25 µL Flash detection reagent (DiscoveRx, Fremont, CA, USA) was added and cells were further incubated for 15 min at 22°C on a table shaker. Luminescence was measured on a Lead Seeker imaging system (GE Healthcare, Chalfont St Giles, Buckinghamshire, UK).

Data analysis and statistical procedures

All data were analysed with GraphPad Prism v5 software. Functional concentration–response curves were fitted to a

three-parameter response model. Intrinsic activity was determined from the fitted graph top values and normalized for agonists to the full histamine response (100%) or for inverse agonists to the thioperamide response (–100%). Statistical differences ($P < 0.05$) between intrinsic activities of subseries of compounds were determined using one-way ANOVA, followed by Dunnett's multiple comparison test.

Fingerprints for Ligands and Proteins three-dimensional quantitative structure–activity relationship (FLAP 3D-QSAR) model building

The dataset used for FLAP 3D-QSAR modelling contained 48 indolecarboxamides with intrinsic activity values ranging from 13 to 100% β-arrestin2 recruitment towards the hH_4R. 3D compound structures were generated from SMILES strings using *Sybyl-X v.1.3* (Sybyl-X, http://www.tripos.com, Tripos International, St. Louis, MO, USA) with a maximum energy threshold of 20 kcal·mol^{-1}. Protonated forms for each molecule at pH 7.4 were generated using an internal tool integrated in FLAP (Baroni *et al.*, 2007), based on the *MoKa* algorithm (Milletti *et al.*, 2007). Stereoisomeric forms were considered for chiral compounds **44**, **53**, **65** and **73**. Subsequently, a FLAP database was instructed to generate a maximum of 50 conformers with RMSD value between two conformers of 0.3 Å and an energy window of 20 kcal·mol^{-1} maximum. Molecular interaction fields (MIFs) were derived from interaction energies with the ligands at specific grid points, as determined by the H (shape), DRY (hydrophobic), N1 (H-bond acceptor) and O (H-bond donor) probes defined in the GRID force field (Goodford, 1985) with a grid spatial resolution of 0.75 Å. Partial least square analysis was used to correlate the MIFs with the intrinsic activities of the different indolecarboxamides. One latent variable (LV1) was set up for the QSAR study as additional components did not lead to either fitting (R^2) or predictivity (Q^2) improvement (data not shown). This means that only one LV was capable of extracting all the information contained in the GRID-MIF descriptors.

Construction of a hH_4R homology model

The hH_4R model was built in homology to the hH_1R crystal structure (Shimamura *et al.*, 2011) and the binding pose of compound **1** was described previously (Schultes *et al.*, 2013). We used the pose of compound **1** as initial binding mode for the other ligands, which were rebuilt using MOE version 2011.10 [Chemical Computing Group (CCG) *MOE (Molecular Operating Environment)*, 2011.10 http://www.chemcomp.com/software.htm]. The models were then subjected to energy minimization using the MMFF94x force field with fixed position of the protein backbone atoms.

Results

Evaluation of indolecarboxamides in a cAMP reporter gene assay

Forty-eight indolecarboxamides (i.e. JNJ 7777120 analogues; see Supporting Information Table S1) and the endogenous agonist histamine were screened ($n = 2$) for their ability to modulate forskolin-induced $G\alpha_i$-dependent CRE activity in hH_4R-expressing cells (Figure 1A). One indolecarboxamide (compound **75**) surprisingly showed positive intrinsic activity of 82 ± 4% compared with full agonist histamine (Eff. 100%). All other compounds including **1** (JNJ 7777120) (Eff. –83 ± 6%) were (weak) inverse agonists (Figure 1A). Full concentration–response curves ($n = 3$) were performed for compound **75** and histamine (Figure 1B). Compound **75** was identified as full agonist (105 ± 5%) with a potency value ($pEC_{50} = 6.4 \pm 0.1$) that equals its affinity ($pK_i = 6.4 \pm 0.1$) (Engelhardt *et al.*, 2012), but is lower than histamine ($pEC_{50} = 8.1 \pm 0.1$) (Figure 1B). To confirm that the observed full agonism of **75** is indeed mediated by the hH_4R, we added increasing concentrations of **1** (JNJ 7777120) to concentration–response curves of **75**. JNJ 7777120 progressively shifted the curves of compound **75** to the right and lowered the basal hH_4R signalling, as can be expected from an inverse agonist (Figure 1C). Schild analysis (slope = 0.9 ± 0.1) showed that **75** and **1** (JNJ 7777120) interact with hH_4R in a competitive manner (Figure 1D). Moreover, the pA_2 (8.5) of **1** (JNJ 7777120) closely resembled its pK_i (8.3) for the hH_4R (Engelhardt *et al.*, 2012).

Activity of indolecarboxamides in a β-arrestin2 recruitment assay

All indolecarboxamides were able to recruit β-arrestin2 to hH_4R. Within our dataset, we could identify compounds with a wide range of potencies ($pEC_{50} = 5.3 \pm 0.1$–8.3 ± 0.1) and intrinsic activities (Eff. = 13 ± 3%–95 ± 4%). Compound **75**, identified above as the only indolecarboxamide that exhibited agonism towards CRE activity, displayed the highest intrinsic activity in recruiting β-arrestin2 to hH_4R (**75**, Eff. = 95 ± 4%). Compound **44** is one of the less effective compounds of the indolecarboxamide series (**44**, Eff. = 14 ± 3%). Substituents at specific positions (R4–R7) on the aromatic ring showed diverse effects on the intrinsic activity of the compounds (**75** vs. **1** vs. **10**), whereas changes in the basic moiety (i.e. methylpiperazine) significantly reduced the intrinsic activity (**49** vs. **73**) (Figure 2).

JNJ 7777120 (**1**) contains a chlorine atom at position R5, which yields an intrinsic activity for β-arrestin recruitment of 62 ± 4%. If this chlorine is replaced with a nitro group (**28**), the resulting intrinsic efficacy (62 ± 4%) is not significantly changed compared with JNJ 7777120 (**1**), whereas moving the nitro group to position R4 is not favoured (**21**, Eff.39 ± 4%) (Figure 3). Interestingly, moving the nitro group to R7, in combination with the chlorine of JNJ 7777120 (**1**) at R5, results in a switch to full agonism in both the $G\alpha_i$ (105 ± 5%) and the β-arrestin (95 ± 4%) pathways (Figure 1A).

Identification of structural features important for potency and intrinsic activity of indolecarboxamides

The indolecarboxamide dataset allows for a detailed investigation of the structural features that are correlated with intrinsic activity to recruit β-arrestin2 to the hH_4R. First, we compared different positions (R4, R5 and R6) of the chlorine atom on the aromatic ring of the indolecarboxamides to the compound without aromatic ring substituents. Addition of a chlorine atom at position R5 is the most favourable in terms

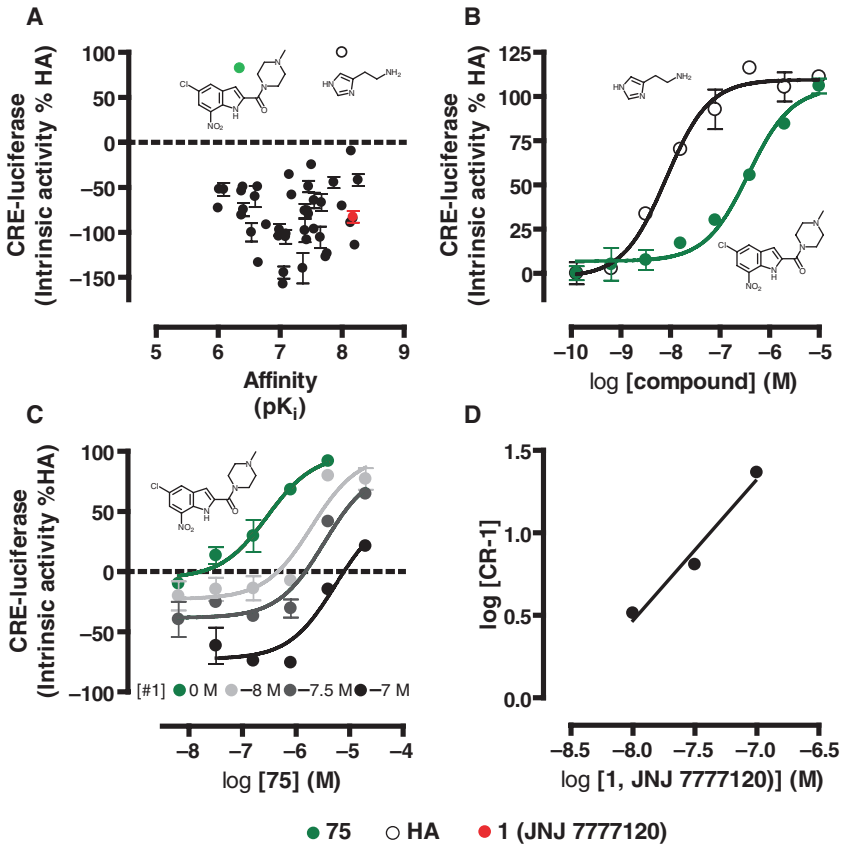

Figure 1

Intrinsic activities of indolecarboxamides in a hH_4R-mediated CRE-luciferase reporter gene assay. hH_4R-mediated inhibition of 1 μM forskolin-stimulated CRE activity in HEK293T cells. HEK293T-hH_4R cells were stimulated with indolecarboxamides (Supporting Information Table S1) (A, 10 μM; B indicated amounts). Intrinsic activity is plotted as percentage of maximal histamine (HA) response. (A) Affinity versus intrinsic activity plot. Structures of agonists are plotted. (B) Concentration–response curves of HA and compound **75**. (C) Concentration–response curves of compound **75** in the absence and presence of increasing amounts of **1** (JNJ 7777120) used to calculate concentration ratios for Schild plot shown in (D). Data shown are pooled data from at least two experiments performed in duplicate. Error bars indicate SD (n = 2) or SEM (n = 3) values.

of intrinsic activity (**1**, Eff. = 62 ± 4%), whereas a chlorine substituent at position R4 (**18**, Eff. = 53 ± 1%) was comparable to the unsubstituted aromatic ring (**10**, Eff. = 47 ± 4%). Although R4 is not the optimal position for the chlorine atom, it does not appear to interfere with the chlorine at R5, with the doubly (R4, R5) substituted compound **48** (Eff. = 63 ± 4.5%) having comparable intrinsic activity to JNJ 7777120 (**1**). However, addition of a chlorine atom at position R6 results in a significant decrease in efficacy (**31**, Eff. = 30 ± 1%) (Figure 4A). The chlorine atom at position R5 displayed the highest potency (**1**, pEC_{50} = 8.0 ± 0.1) and the chlorine at position R6 the lowest potency (**31**, pEC_{50} = 6.8 ± 0.1) in this subseries.

Next, different substituents were evaluated at position R5. A chlorine atom (**1**, Eff. = 62 ± 4%) or a nitro group (**28**, Eff. = 62 ± 4%) showed the highest intrinsic activity and an amine group (**29**, Eff. = 57 ± 3%) was also tolerated. Larger substituents at position R5, such as a methoxy group, were less favourable and showed a significant loss in intrinsic activity (**26**, Eff. = 44 ± 6%) and moreover a 400-fold decrease in potency compared to **1** (Figure 4B). In addition, potency values for **28** (pEC_{50} = 7.0 ± 0.0) and **29** (pEC_{50} = 7.4 ± 0.1) decreased more than fourfold compared to **1** (pEC_{50} = 8.0 ± 0.1).

We have previously demonstrated (Figure 3) that addition of a nitro group into R7 results in a significant increase in intrinsic activity compared to the unsubstituted compound JNJ 7777120 (**1**). When we further explored this position, we found that substituting this nitro group with either methyl (**50**, Eff. = 63 ± 4%), amine (**51**, Eff. = 58 ± 4%) or a fluor atom (**49**, Eff. = 57 ± 2%), resulted in activity comparable to JNJ 7777120 (**1**), demonstrating that there is very steep SAR at this position and only the nitro group is able to increase intrinsic activity. Interestingly, although the nitro group resulted in higher intrinsic efficacy, this was coupled with a loss in potency (**75**, pEC_{50} = 6.0 ± 0.1) compared to the other compounds in this subseries (pEC_{50} = 7.8–8.2).

Finally, we evaluated the effect of different basic side chain structures on the intrinsic activity of indolecarboxamides to recruit β-arrestin2. Compound **49** has a methylpiperazine side chain and demonstrated highest intrinsic activity in this subseries (Eff. = 57 ± 2%). Replacement of this methylpiperazine with a piperazine ring (**74**) had very little effect on intrinsic activity (Eff. = 50 ± 0%), whereas substitutions with azetidin-3-yl pyrrolidine (**71**, Eff. = 35 ± 1%), 3-aminomethyl azetidine (**72**, Eff. = 37 ± 3%), 4-methyl-1,4-diazepane (**69**, Eff. = 36 ± 2%) or 3-aminomethyl pyrrolidine (**73**, Eff. = 19 ±

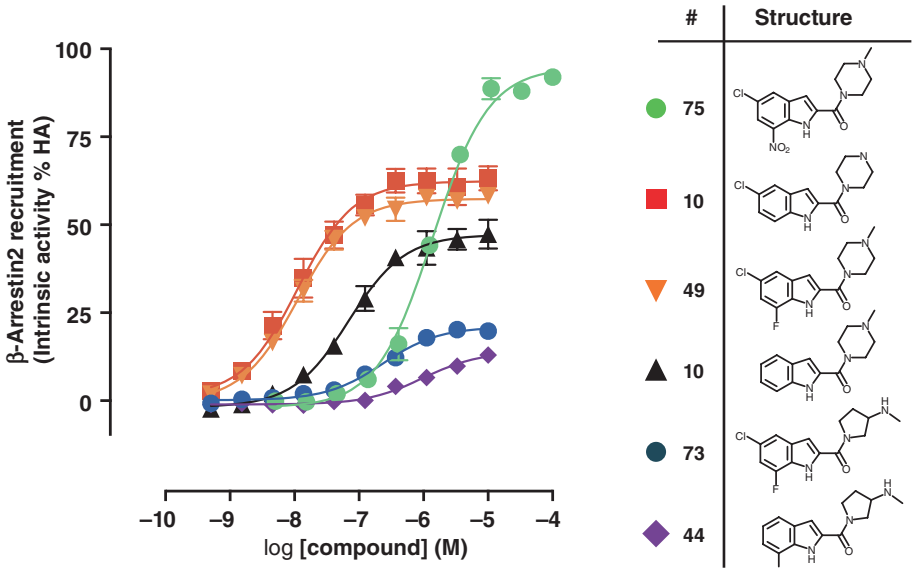

Figure 2

Indolecarboxamides exhibit a wide range of intrinsic activities in inducing β-arrestin2 recruitment. U2OS-H_4R cells were stimulated with increasing amounts of indicated compounds. Intrinsic activity is plotted as percentage of maximal histamine (HA) response. Data shown are pooled data from at least three experiments performed in duplicate. Error bars indicate SEM values.

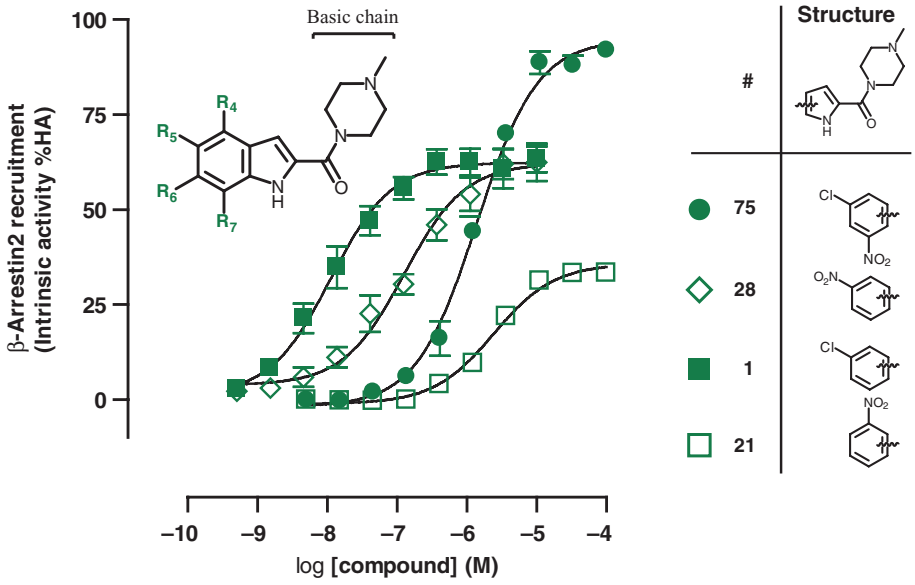

Figure 3

Effect of nitro substituent on β-arrestin2 intrinsic activity. U2OS-H_4R cells were stimulated with indicated amount of indolecarboxamides to evaluate the effect of NO_2 substituents at different positions. Intrinsic activity is plotted as percentage of maximal histamine (HA) response. Data shown are pooled data from at least three experiments performed in duplicate. Error bars indicate SEM values.

5%), all resulted in a significant decrease in intrinsic activity (Figure 4D). The methylpiperazine side chain (**1**, pEC_{50} = 8.0 ± 0.1) also resulted in the highest potency. Compound **71** has a 10-fold higher potency (**71**, pEC_{50} = 7.2 ± 0.1) than **72** and **69** (**72**, pEC_{50} = 6.2 ± 0.1 and **69**, pEC_{50} = 6.2 ± 0.1) to induce β-arrestin2 recruitment to hH_4R. In addition, when other substituents were present on the aromatic ring (**55**, **63**, **46**), changes in the basic side chain resulted in similar intrinsic activity decreases (Supporting Information Figure S1), indicating an important role for this basic side chain of hH_4R ligands to induce β-arrestin2 signalling.

Potency values of all tested indolecarboxamides to stimulate β-arrestin2 recruitment to hH_4R are linearly correlated with their hH_4R binding affinity values that we previously

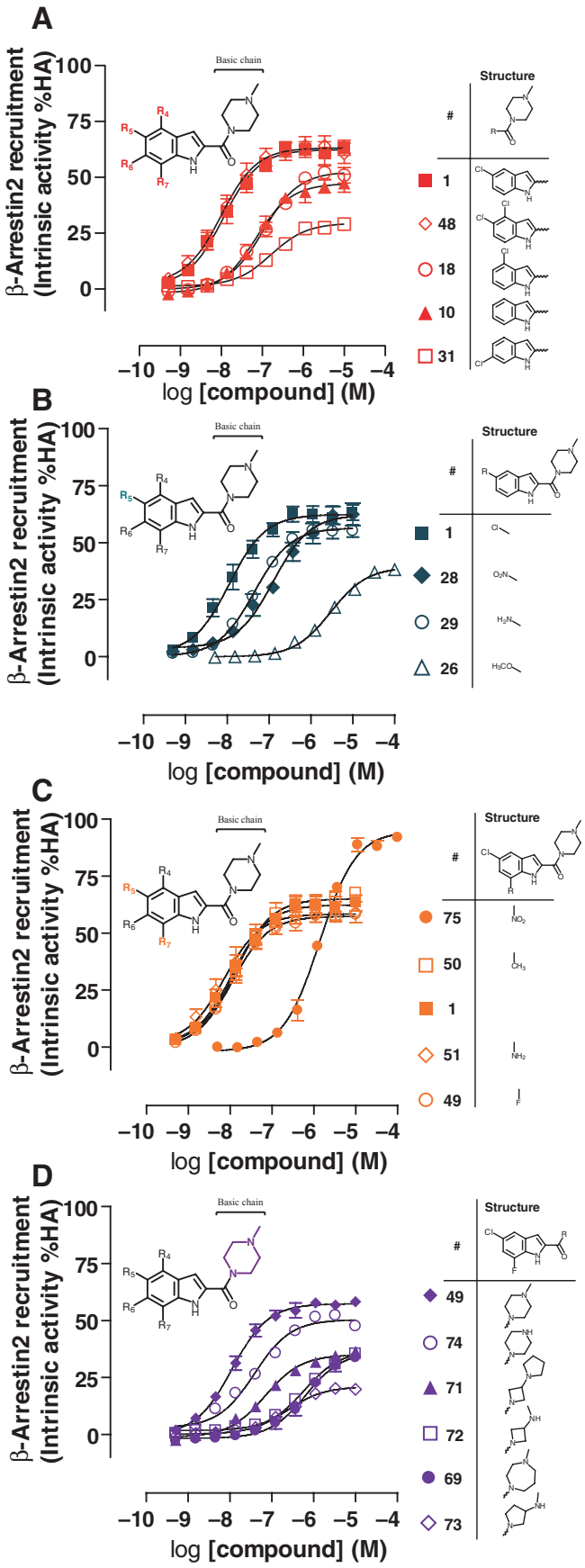

Figure 4

Structural features of indolecarboxamides influence compound intrinsic activity in β-arrestin2 recruitment. U2OS-H_4R cells were stimulated with indicated amount of indolecarboxamides. (A) Chlorine substituent at different positions. (B) Different substituents at R5 position. (C) Different substituents at R7 position. (D) Effect of different basic side chains. Intrinsic activity is plotted as percentage of maximal histamine (HA) response. Data shown are pooled data from at least three experiments performed in duplicate. Error bars indicate SEM values.

reported (Engelhardt *et al.*, 2012) (slope = 1.1 ± 0.1, R^2 = 0.89) (Figure 5A). In contrast, no correlation was observed between intrinsic activity and affinity values (Figure 5B).

Unravelling ligand interaction regions by FLAP-3D-QSAR

The dataset presented in Figures 2–4 were analysed using FLAP 3D-QSAR computational-based analysis (Baroni *et al.*, 2007). Four-point pharmacophores (quadruplets) derived from MIFs (Goodford, 1985) were used to align JNJ 7777120 and its analogues **2–77** for the construction of a FLAP 3D-QSAR model (Figure 6A). MIF hotspots derived from this analysis revealed essential molecular interaction features that are either favourable or unfavourable for the intrinsic activity of indolecarboxamides to recruit β-arrestin2 to the hH_4R. The correlation plot of experimental versus predicted intrinsic activity values (R^2 = 0.76; Q^2 = 0.51) showed three outliers (i.e. **31**, **35** and **75**) (Figure 6B, red dots). These outliers can be explained by the very low variability of the SAR space on position R6 (**31** and **35**), while for compound **75**, the cause probably lies in the large efficacy gap between **75** and the remaining dataset compounds, as well as the fact that this compound is the only unbiased compound of the series. The three outliers were therefore excluded from the analysis and a new intrinsic activity model was computed (Figure 6B, blue dotted lines) that displayed a better fit and higher predictive performance (R^2 = 0.89; Q^2 = 0.71). 3D pictures of compounds **1** and **44** that display high (Eff. = 62 ± 4%; Figure 6C) and low (Eff. = 14 ± 3%; Figure 6D) intrinsic activity, respectively, were constructed to illustrate the intrinsic activity hotspots by defining positive and negative ligand features (surfaces). The longer basic side chain of **44** places the hydrogen bond donor in a suboptimal position (Figure 6D). Substituents at the R4 and R5 position (**1**) are positively correlated (shape) with intrinsic activity. Hydrophobic substituents are favourable at position R5 (Figure 6C). However, substituents at position R7 (**44**) are unfavourable (shape and hydrophobic) for activity (Figure 6D).

Indolecarboxamide binding in the hH_4R binding pocket

We constructed hH_4R models with unbiased compound **75** (Figure 7A), high biased β-arrestin2 activity compound **1** (Figure 7B) and low biased β-arrestin2 activity compound **44** (Figure 7C) in order to translate the identified ligand intrinsic activity features to molecular interactions with the hH_4R binding pocket. We observed a clear interaction of the basic nitrogen of the methylpiperazine (**1** and **75**) and 3-aminomethyl pyrrolidine (**44**) with $D^{3.32}$ in TM3, which is a

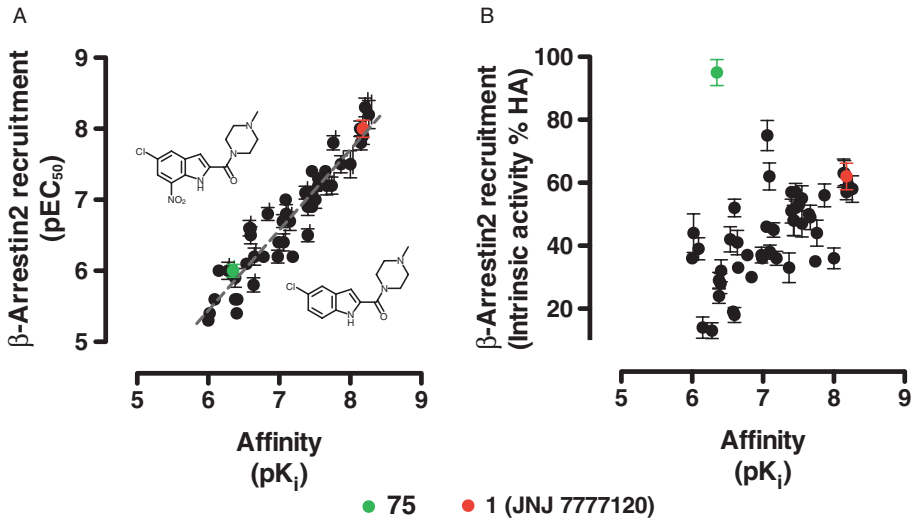

Figure 5

Correlation plots between affinity, potency and intrinsic activity in a β-arrestin2 recruitment assay. (A) Linear correlation between affinity and β-arrestin2 recruitment assay potency values. Linear regression line is shown as grey dotted line. (B) No correlation was found between affinity and intrinsic activity in a β-arrestin2 recruitment assay. Data shown are pooled data from at least three experiments performed in duplicate. Error bars indicate SEM values. HA, histamine.

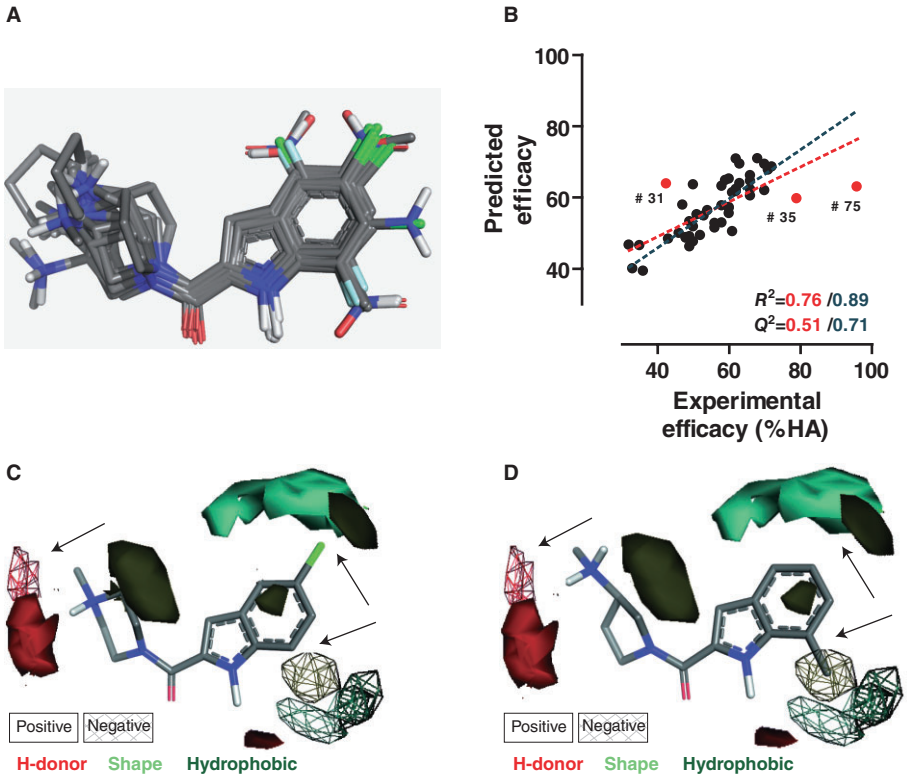

Figure 6

FLAP QSAR analysis of the indolecarboxamides intrinsic activity in β-arrestin2 recruitment. (A) Alignment of the 48 tested indolecarboxamides based on molecular interaction fields. (B) Correlation plot between experimental and predicted intrinsic activity values. Regression lines were fitted in the presence (red) or absence (blue) of outliers (see text for details). (C, D) FLAP 3D-QSAR models with high intrinsic activity compound **1** (C) or low intrinsic activity compound **44** (D). Shown surfaces represent positive (solid) or negative (grating) effects of shape, H-bond donor or hydrophobic ligand features. Arrows indicate the most remarkable differences between (C) and (D). HA, histamine.

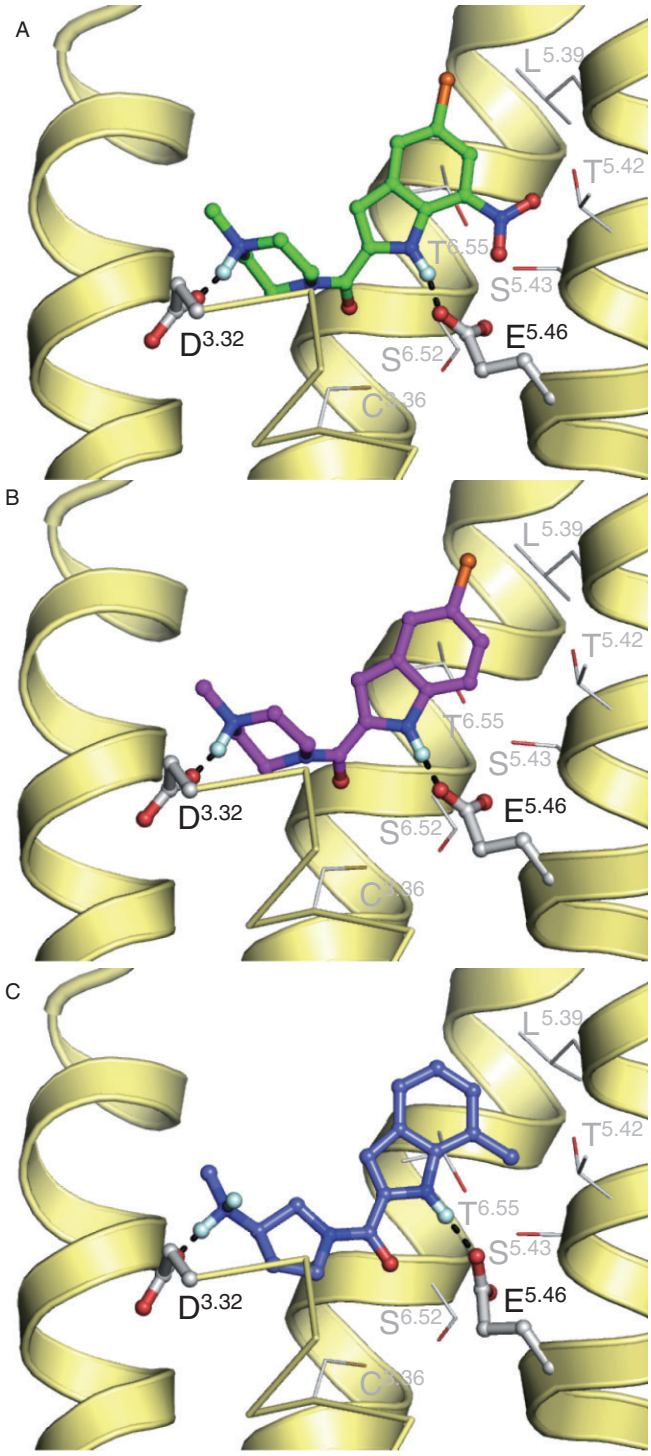

Figure 7

Three indolecarboxamides fitted in the hH_4R binding pocket. (A) Compound **75**, (B) compound **1** (JNJ 7777120) and (C) compound **44**. Compounds are depicted as ball-and-sticks. Important pocket residues are shown as lines, whereas $D^{3.32}$ and $E^{5.46}$ that both form H-bonds with the ligands are also shown as ball-and-sticks. H-bonds between the ligand and pocket residues are represented as black dotted lines. The backbone TM helices 5, 6 and 7 (right to left) are presented as yellow helices. For clarity, helix 3 is partly presented by yellow ribbons.

key for histamine and JNJ 7777120 binding, as determined in previous studies (Shin *et al.*, 2002; Jongejan *et al.*, 2008). In addition, an interaction between the indole nitrogen with $E^{5.46}$ in TM5 is most likely to occur and consequently points the aromatic ring towards the hydrophobic cavity at the extracellular side of the hH_4R (Jongejan *et al.*, 2008; Lim *et al.*, 2010; Istyastono *et al.*, 2011; Schultes *et al.*, 2013). The nitro group of compound **75** seems to be directed towards TM5 and the chlorine atom is pointing slightly more upwards towards the extracellular side as compared to **1** (JNJ 7777120). The distance from the positively charged nitrogen in the pyrrolidine to the indole nitrogen (compound **44**) is longer than for the respective methylpiperazine derivatives (e.g. **1**), which resulted in a different positioning of the aromatic ring. Due to the hydrophobic methyl group at position R7, the aromatic ring is pointed more upwards and less in proximity to TM5 than the nitro substituent of compound **75** at this position (Figure 7).

Discussion and conclusion

Despite the recent progress in GPCR structural biology and the current availability of both inactive and active GPCR structures (Palczewski *et al.*, 2000; Jaakola *et al.*, 2008; Park *et al.*, 2008; Warne *et al.*, 2008; Wu *et al.*, 2010; Rosenbaum *et al.*, 2011; Shimamura *et al.*, 2011; Manglik *et al.*, 2012), it is still challenging to successfully predict ligand interaction points and efficacy switches. The recent evidence for multiple active GPCR states (Kahsai *et al.*, 2011; Kenakin, 2011) has added additional complexity and the molecular understanding of ligand-biased GPCR activation can be considered as one of the challenges in the field. Previously, we identified several biased ligands for the hH_4R (Rosethorne and Charlton, 2011; Nijmeijer *et al.*, 2012). Although this biased activity seemed to be spread among different ligand classes, all five investigated indolecarboxamides showed a full bias toward β-arrestin2 recruitment. In this study, we tested 48 indolecarboxamides with subtle structural differences in aromatic ring substituents and in the basic side chain (Engelhardt *et al.*, 2012). The 47 β-arrestin2-biased indolecarboxamides displayed a wide variation in potencies and intrinsic activities. The potencies correlated with previously published affinities (Engelhardt *et al.*, 2012), which is in line with earlier observations that β-arrestin2 signalling is correlated with receptor occupancy and in line with the 1:1 stoichiometry of receptor and β-arrestin2 interaction in an enzyme fragment-based complementation assay (Granier *et al.*, 2012; Kruse *et al.*, 2012; Riddy *et al.*, 2012; Shoichet and Kobilka, 2012). No correlation was observed between affinity and intrinsic activities, making it worthwhile to identify the structural requirements for intrinsic activity.

In a $G\alpha_i$ protein-dependent reporter gene assay, compound **75** was the only compound that displayed agonism. Intriguingly, this compound exhibited also the highest intrinsic activity in the β-arrestin2 recruitment assay and is therefore classified as an unbiased ligand. Interestingly, the polar nitro group at position R7 did not match with the negative H (shape) MIF coefficient in the constructed β-arrestin2-biased ligand intrinsic activity model. This could be explained by the fact that compound **75** is the only unbi-

ased indolecarboxamide of this series and we hypothesize that **75** recruits β-arrestin2 to hH_4R by potentially stabilizing a distinct receptor conformation as compared with the other indolecarboxamides.

Using the binding mode of indolecarboxamides in the hH_4R that was previously proposed and validated with site-directed mutagenesis data (Jongejan *et al.*, 2008; Schultes *et al.*, 2013) as well as with the recently successfully applied FLAP method [hH_3R, CXCR7 and calcium channel compounds (Ioan *et al.*, 2012; Sirci *et al.*, 2012; Wijtmans *et al.*, 2012)] for 3D-QSAR, we now identified receptor regions important for ligand efficacy. In the histamine H_3R, it was previously shown that the length between the charged groups in the ligand is important for intrinsic activity (Govoni *et al.*, 2006). Because of the crucial interaction between $D^{3.32}$ and the basic nitrogen in the side chain of the indolecarboxamides, the position of the aromatic ring depends on the distance between this basic nitrogen and the indole nitrogen. Besides the length, also the different substitutions at the aromatic ring are responsible for this ring placement in the binding pocket. The nitro group at position R7 of unbiased indolecarboxamide **75** seems able to form hydrogen bonds with threonine and serine residues in transmembrane (TM) 5, which is possibly a crucial step in hH_4R $G\alpha_i$ activation. Notably, these polar interactions cannot take place for **1** and **44**. Interestingly, compound **51** that has an amine group at R7 does not show agonism in the $G\alpha_i$ pathway, which could indicate that the polar interactions are made via a hydrogen bond-accepting group in the ligand.

There are multiple theories for GPCR activation mechanisms and most of them focus on the rearrangement of TM helices such as 5, 6 and 7 in combination with aromatic side chain rotamer switches (Ballesteros *et al.*, 2000; Schwartz *et al.*, 2006). The efficacy of dopamine D_1 agonists for cAMP stimulation has been correlated with ligand interactions with a series in TM5 (Chemel *et al.*, 2012). For the β_2 adrenergic receptor (ADRB2), interaction with $D^{3.32}$ and an inward shift of TM5 was required for agonist activity as demonstrated by strong polar interactions between ligand and residues in TM5 (Strader *et al.*, 1989; Liapakis *et al.*, 2000; Rasmussen *et al.*, 2011a; Zocher *et al.*, 2012) as well as an interaction between $S^{5.43}$ and $N^{6.55}$ (Katritch *et al.*, 2009; Vilar *et al.*, 2011). Interestingly, these polar interactions with TM5 could be confirmed in the recent crystal structure models (Rosenbaum *et al.*, 2011). In contrast, no TM5 movement was observed in the $A_{2A}AR$, indicating that TM5 interactions are not a general phenomenon (Katritch and Abagyan, 2010). We recently suggested that agonist binding results in hH_1R activation via $S^{3.36}$, a rotamer toggle switch that initiates activation via $N^{7.45}$ resulting in conformational changes in helices 6 and 7 (Jongejan *et al.*, 2005). In addition, agonist binding disrupts the $T^{3.37}$ interaction with TM5, which resulted in a $P^{5.50}$-induced unwinding of the TM5 helix around the side chain $I^{3.40}$ (Sansuk *et al.*, 2011). Shortly after the discovery of the hH_4R, $D^{3.32}$ and $E^{5.46}$ were identified as key residues for ligand binding and activation (Shin *et al.*, 2002). The residues $T^{5.42}$ and $S^{5.43}$ in TM5 of hH_4R were not significantly involved in histamine binding or activation, but $N^{4.57}$ and $S^{6.52}$ played a role in receptor activation (Shin *et al.*, 2002). More recently, $N^{4.57}$ was shown to play a role in the binding of clobenpropit analogue VUF5228 (Istyastono *et al.*, 2011) and was identified as the key determinant for ligand binding to H_4R orthologs through its influence on the orientation of $E^{5.46}$ (Lim *et al.*, 2010). In addition, mutation of this $N^{4.57}$ residue as well as $S^{5.43}$ decreased the affinity of JNJ 7777120. The possible interaction of **75** with polar hH_4R receptor residues is currently under investigation.

Based on our dataset, we observed that β-arrestin2 activation of the tested indolecarboxamides is less dependent on such polar interactions than $G\alpha_i$ protein signalling. In a previous quantitative structure–*affinity* relationship study, the position R7 tolerated both lipophilic and polar moieties (Engelhardt *et al.*, 2012). Yet, in the present study, we show that (hydrophobic) substituents at this position are less favourable for biased β-arrestin2 recruitment. This illustrates that there are specific intrinsic activity hotspots that do not correspond with high affinity features. Substitutions (i.e. halogens or hydrophobic groups) on positions R6 or R7 seem to repulse the ligand from the TM5 region in the hH_4R homology model, resulting in a lower intrinsic activity. Furthermore, the replacement of methylpiperazine with other basic side chains was found to be detrimental for intrinsic activity. With our FLAP 3D-QSAR model, we could identify an exact hotspot, namely the correct positioning of the H-bond donor MIF generated by the positively charged nitrogen in the basic side chain, which interacts with $D^{3.32}$ in the H_4R homology model. Consequently, variations in the basic side chain resulted in a slightly different orientation of the aromatic ring. Based on the hH_4R homology model, we observed that the less effective compounds seem to point their aromatic ring more upwards to the extracellular side of hH_4R and less towards the TM5 region, hence probably resulting in decreased β-arrestin2 recruitment.

In this study, we have identified ligand and receptor features responsible for biased hH_4R signalling by testing 48 indolecarboxamides with subtle structural differences. We discovered an unbiased indolecarboxamide (**75**) that is a full agonist in both $G\alpha_i$ protein and β-arrestin2 signalling. All other compounds displayed a full bias toward β-arrestin2 recruitment. An extensive analysis of the ligand structures and corresponding intrinsic activity via a FLAP 3D-QSAR model revealed β-arrestin2-biased activity hotspots, which were subsequently projected in a hH_4R homology model to identify receptor regions that play a role in biased signalling. Importantly, while a hydrogen bond acceptor that points towards the TM5 region is crucial for $G\alpha_i$-protein signalling, this polar interaction is not necessary to induce β-arrestin2 recruitment by fully biased ligands. In the latter case, intrinsic activity is probably dependent on subtle changes in orientation of the aromatic ring in the hydrophobic sub-pocket. Identification of molecular features that are essential for (biased) ligands is important to predict compound intrinsic activity and allows the rational design of biased and unbiased hH_4R ligands.

Acknowledgements

S. N., H. F. V., C. d. G. and R. L. participate in the European COST Action BM0806. C.d. G. is supported by The Netherlands Organization for Scientific Research NWO: VENI Grant 700.59.408. We thank Molecular Discovery Ltd. for granting FLAP suite licence.

Conflict of interest

None.

References

Ballesteros JA, Deupi X, Olivella M, Haaksma EEJ, Pardo L (2000). Serine and threonine residues bend alpha-helices in the chi(1) = g(-) conformation. Biophys J 79: 2754–2760.

Baroni M, Cruciani G, Sciabola S, Perruccio F, Mason JS (2007). A common reference framework for analyzing/comparing proteins and ligands. Fingerprints for Ligands and Proteins (FLAP): theory and application. J Chem Inf Model 47: 279–294.

Bohn LM, McDonald PH (2010). Seeking ligand bias: assessing GPCR coupling to beta-arrestins for drug discovery. Drug Discov Today Technol 7: e37–e42.

Chemel BR, Bonner LA, Watts VJ, Nichols DE (2012). Ligand specific roles for transmembrane 5 serine residues in the binding and efficacy of dopamine D (1) receptor catachol agonists. Mol Pharmacol 81: 729–738.

Coge F, Guenin SP, Rique H, Boutin JA, Galizzi JP (2001). Structure and expression of the human histamine H4-receptor gene. Biochem Biophys Res Commun 284: 301–309.

DeWire SM, Violin JD (2011). Biased ligands for better cardiovascular drugs: dissecting G-protein-coupled receptor pharmacology. Circ Res 109: 205–216.

Engelhardt H, de Esch IJ, Kuhn D, Smits RA, Zuiderveld OP, Dobler J *et al.* (2012). Detailed structure-activity relationship of indolecarboxamides as H4 receptor ligands. Eur J Med Chem 54: 660–668.

Galandrin S, Oligny-Longpre G, Bouvier M (2007). The evasive nature of drug efficacy: implications for drug discovery. Trends Pharmacol Sci 28: 423–430.

Goodford PJ (1985). A computational procedure for determining energetically favorable binding sites on biologically important macromolecules. J Med Chem 28: 849–857.

Govoni M, Lim HD, El-Atmioui D, Menge WM, Timmerman H, Bakker RA *et al.* (2006). A chemical switch for the modulation of the functional activity of higher homologues of histamine on the human histamine H3 receptor: effect of various substitutions at the primary amino function. J Med Chem 49: 2549–2557.

Granier S, Manglik A, Kruse AC, Kobilka TS, Thian FS, Weis WI *et al.* (2012). Structure of the δ-opioid receptor bound to naltrindole. Nature 485: 400–404.

Haga K, Kruse AC, Asada H, Yurugi-Kobayashi T, Shiroishi M, Zhang C *et al.* (2012). Structure of the human M2 muscarinic acetylcholine receptor bound to an antagonist. Nature 482: 547–551.

Ioan P, Ciogli A, Sirci F, Budriesi R, Cosimelli B, Pierini M *et al.* (2012). Absolute configuration and biological profile of two thiazinooxadiazol-3-ones with L-type calcium channel activity: a study of the structural effects. Org Biomol Chem 10: 8994–9003.

Istyastono EP, Nijmeijer S, Lim HD, van de Stolpe A, Roumen L, Kooistra AJ *et al.* (2011). Molecular determinants of ligand binding modes in the histamine H(4) receptor: linking ligand-based three-dimensional quantitative structure-activity relationship (3D-QSAR) models to in silico guided receptor mutagenesis studies. J Med Chem 54: 8136–8147.

Jaakola VP, Griffith MT, Hanson MA, Cherezov V, Chien EY, Lane JR *et al.* (2008). The 2.6 angstrom crystal structure of a human A2A adenosine receptor bound to an antagonist. Science 322: 1211–1217.

Jongejan A, Bruysters M, Ballesteros JA, Haaksma E, Bakker RA, Pardo L *et al.* (2005). Linking agonist binding to histamine H1 receptor activation. Nat Chem Biol 1: 98–103.

Jongejan A, Lim HD, Smits RA, de Esch IJ, Haaksma E, Leurs R (2008). Delineation of agonist binding to the human histamine H4 receptor using mutational analysis, homology modeling, and *ab initio* calculations. J Chem Inf Model 48: 1455–1463.

Kahsai AW, Xiao K, Rajagopal S, Ahn S, Shukla AK, Sun J *et al.* (2011). Multiple ligand-specific conformations of the β2-adrenergic receptor. Nat Chem Biol 7: 692–700.

Katritch V, Abagyan R (2010). GPCR agonist binding revealed by modeling and cristallography. Trends Pharmacol Sci 32: 637–643.

Katritch V, Reynolds KA, Cherezov V, Hanson MA, Roth CB, Yeager M *et al.* (2009). Analysis of full and partial agonists binding to beta2 adrenergic receptor suggests a role of transmembrane helix V in agonist-specific conformational changes. J Mol Recognit 22: 307–318.

Kenakin T (2003). Ligand-selective receptor conformations revisited: the promise and the problem. Trends Pharmacol Sci 24: 346–354.

Kenakin T (2011). Functional selectivity and biased receptor signaling. J Pharmacol Exp Ther 336: 296–302.

Kruse AC, Hu J, Pan AC, Arlow DH, Rosenbaum DM, Rosemond E *et al.* (2012). Structure and dynamics of the M3 muscarinic acetylcholine receptor. Nature 482: 552–556.

Leurs R, Chazot PL, Shenton FC, Lim HD, de Esch IJ (2009). Molecular and biochemical pharmacology of the histamine H4 receptor. Br J Pharmacol 157: 14–23.

Liapakis G, Ballesteros JA, Papachristou S, Chan WC, Chen X, Javitch JA (2000). The forgotten serine. A critical role for Ser-203 5.42 in ligand binding to and activation of the beta2 adrenergic receptor. J Biol Chem 275: 37779–37788.

Lim HD, de Graaf C, Jiang W, Sadek P, McGovern PM, Istyastono EP *et al.* (2010). Molecular determinants of ligand binding to H4R species variants. Mol Pharmacol 77: 734–743.

Liu C, Ma X, Jiang X, Wilson SJ, Hofstra CL, Blevitt J *et al.* (2001). Cloning and pharmacological characterization of a fourth histamine receptor (H(4)) expressed in bone marrow. Mol Pharmacol 59: 420–426.

Manglik A, Kruse AC, Kobilka TS, Thian FS, Mathiesen JM, Sunahara RK *et al.* (2012). Crystal structure of the μ-opioid receptor bound to a morphinan antagonist. Nature 485: 321–326.

Milletti F, Storchi L, Sforna G, Cruciani G (2007). New and original pKa prediction method using grid molecular interaction fields. J Chem Inf Model 47: 2172–2181.

Morse KL, Behan J, Laz TM, West RE, Jr, Greenfeder SA, Anthes JC *et al.* (2001). Cloning and characterization of a novel human histamine receptor. J Pharmacol Exp Ther 296: 1058–1066.

Nakamura T, Itadani H, Hidaka Y, Ohta M, Tanaka K (2000). Molecular cloning and characterization of a new human histamine receptor, HH4R. Biochem Biophys Res Commun 279: 615–620.

Nijmeijer S, Vischer HF, Rosethorne EM, Charlton SJ, Leurs R (2012). Analysis of multiple histamine H4 receptor compound classes uncovers Gαi and β-arrestin2-biased ligands. Mol Pharmacol 82: 1174–1182.

Oda T, Morikawa N, Saito Y, Masuho Y, Matsumoto S (2000). Molecular cloning and characterization of a novel type of histamine receptor preferentially expressed in leukocytes. J Biol Chem 275: 36781–36786.

Palczewski K, Kumasaka T, Hori T, Behnke CA, Motoshima H, Fox BA *et al.* (2000). Crystal structure of rhodopsin: a G protein-coupled receptor. Science 289: 739–745.

Park JH, Scheerer P, Hofmann KP, Choe HW, Ernst OP (2008). Crystal structure of the ligand-free G-protein-coupled receptor opsin. Nature 454: 183–187.

Rajagopal S, Rajagopal K, Lefkowitz RJ (2010). Teaching old receptors new tricks: biasing seven-transmembrane receptors. Nat Rev Drug Discov 9: 373–386.

Rasmussen SG, Choi HJ, Fung JJ, Pardon E, Casarosa P, Chae PS *et al.* (2011a). Structure of a nanobody-stabilized active state of the β(2) adrenoceptor. Nature 469: 175–180.

Rasmussen SG, DeVree BT, Zou Y, Kruse AC, Chung KY, Kobilka TS *et al.* (2011b). Crystal structure of the β2 adrenergic receptor-Gs protein complex. Nature 477: 549–555.

Reiter E, Ahn S, Shukla AK, Lefkowitz RJ (2012). Molecular mechanism of β-arrestin-biased agonism at seven-transmembrane receptors. Annu Rev Pharmacol Toxicol 52: 179–197.

Riddy DM, Stamp C, Sykes DA, Charlton SJ, Dowling MR (2012). Reassessment of the pharmacology of Sphingosine-1-phosphate S1P3 receptor ligands using the DiscoveRx PathHunter™ and Ca2+ release functional assays. Br J Pharmacol 167: 868–880.

Rosenbaum DM, Zhang C, Lyons JA, Holl R, Aragao D, Arlow DH *et al.* (2011). Structure and function of an irreversible agonist-β(2) adrenoceptor complex. Nature 469: 236–240.

Rosethorne EM, Charlton SJ (2011). Agonist-biased signaling at the histamine H4 receptor: JNJ7777120 recruits β-arrestin without activating G proteins. Mol Pharmacol 79: 749–757.

Sansuk K, Deupi X, Torrecillas IR, Jongejan A, Nijmeijer S, Bakker RA *et al.* (2011). A structural insight into the reorientation of transmembrane domains 3 and 5 during family A G protein-coupled receptor activation. Mol Pharmacol 79: 262–269.

Schultes S, Nijmeijer S, Engelhardt H, Kooistra AJ, Vischer HF, de Esch IJP *et al.* (2013). Mapping histamine H4 receptor–ligand binding modes. MedChemComm 4: 193–204.

Schwartz TW, Frimurer TM, Holst B, Rosenkilde MM, Elling CE (2006). Molecular mechanism of 7TM receptor activation – a global toggle switch model. Annu Rev Pharmacol Toxicol 46: 481–519.

Shimamura T, Shiroishi M, Weyand S, Tsujimoto H, Winter G, Katritch V *et al.* (2011). Structure of the human histamine H1 receptor complex with doxepin. Nature 475: 65–70.

Shin N, Coates E, Murgolo NJ, Morse KL, Bayne M, Strader CD *et al.* (2002). Molecular modeling and site-specific mutagenesis of the histamine-binding site of the histamine H4 receptor. Mol Pharmacol 62: 38–47.

Shoichet BK, Kobilka BK (2012). Structure-based drug screening for G-protein-coupled receptors. Trends Pharmacol Sci 33: 268–272.

Sirci F, Istyastono EP, Vischer HF, Kooistra AJ, Nijmeijer S, Kuijer M *et al.* (2012). Virtual fragment screening: discovery of histamine H(3) receptor ligands using ligand-based and protein-based molecular fingerprints. J Chem Inf Model 52: 3308–3324.

Strader CD, Sigal JS, Dixon RA (1989). Structural basis of beta adrenergic receptor function. FASEB J 3: 1825–1832.

Thurmond RL, Desai PJ, Dunford PJ, Fung-Leung WP, Hofstra CL, Jiang W *et al.* (2004). A potent and selective histamine H4 receptor antagonist with anti-inflammatory properties. J Pharmacol Exp Ther 309: 404–413.

Vilar S, Karpiak J, Berk B, Costanzi S (2011). In silico analysis of the binding of agonists and blockers to the beta2 adrenergic receptor. J Mol Graph Model 29: 809–817.

Violin JD, DeWire SM, Yamashita D, Rominger DH, Nguyen L, Schiller K *et al.* (2010). Selectively engaging β-arrestins at the angiotensin II type 1 receptor reduces blood pressure and increases cardiac performance. J Pharmacol Exp Ther 335: 572–579.

Warne T, Serrano-Vega MJ, Baker JG, Moukhametzianov R, Edwards PC, Henderson R *et al.* (2008). Structure of a beta1-adrenergic G-protein-coupled receptor. Nature 454: 486–491.

Wijtmans M, Maussang D, Sirci F, Scholten DJ, Canals M, Mujic-Delic A *et al.* (2012). Synthesis, modeling and functional activity of substituted styrene-amides as small-molecule CXCR7 agonists. Eur J Med Chem 51: 184–192.

Wu B, Chien EY, Mol CD, Fenalti G, Liu W, Katritch V *et al.* (2010). Structures of the CXCR4 chemokine GPCR with small-molecule and cyclic peptide antagonists. Science 330: 1077–1071.

Zampeli E, Tiligada E (2009). The role of histamine H4 receptor in immune and inflammatory disorders. Br J Pharmacol 157: 24–33.

Zhu Y, Michalovich D, Wu H, Tan KB, Dytko GM, Mannan IJ *et al.* (2001). Cloning, expression, and pharmacological characterization of a novel human histamine receptor. Mol Pharmacol 59: 434–441.

Zocher M, Fung JJ, Kobilka BK, Muller DJ (2012). Ligand-specific interactions modulate kinetic, energetic, and mechanical properties of the human β2 adrenergic receptor. Structure 20: 1391–1402.

Supporting information

Additional Supporting Information may be found in the online version of this article at the publisher's web-site:

Figure S1 Effect of different basic side chains influences compound intrinsic activity in β-arrestin2 recruitment. U2OS-H_4R cells were stimulated with indicated amount of indolecarboxamides. (A) R5-Cl, R7-CH_3 (B) R7-F (C) R7-CH_3. Intrinsic activity is plotted as percentage of maximal histamine (HA) response. Data shown are pooled data from at least three experiments performed in duplicate. Error bars indicate SEM values.

Table S1 Overview of potency and intrinsic activity values in a β-arrestin2 recruitment and CRE-luciferase assay. Intrinsic activity is calculated as percentage of maximal histamine (HA) response. Data shown are pooled data from at least three experiments performed in duplicate. Error bars indicate SEM values.